

One-magnon Raman scattering in La_2CuO_4 : The origin of the field-induced mode

M. B. Silva Neto^{1,*} and L. Benfatto²

¹*Institute for Theoretical Physics, University of Utrecht, P.O. Box 80.195, 3508 TD, Utrecht, The Netherlands*

²*CNR-SMC-INFN and Department of Physics, University of Rome "La Sapienza," Piazzale Aldo Moro 5, 00185 Rome, Italy*

(Received 6 July 2005; revised manuscript received 2 September 2005; published 4 October 2005)

We investigate the one-magnon Raman scattering in the layered antiferromagnetic La_2CuO_4 compound. We find that the Raman signal is composed by two one-magnon peaks: one in the B_{1g} channel, corresponding to the Dzyaloshinskii-Moryia mode, and another in the B_{3g} channel, corresponding to the XY mode. Furthermore, we show that a peak corresponding to the XY mode can be induced in the planar (RR) geometry when a magnetic field is applied along the easy axis for the sublattice magnetization. The appearance of such a field-induced mode signals the existence of a *magnetic state* above the Néel temperature T_N , where the direction of the weak-ferromagnetic moment lies within the CuO_2 planes.

DOI: [10.1103/PhysRevB.72.140401](https://doi.org/10.1103/PhysRevB.72.140401)

PACS number(s): 75.10.Jm, 74.25.Ha, 75.30.Gw, 87.64.Je

The possibility of inelastic light scattering by one- and two-magnon excitations in magnetic insulators was acknowledged long ago by Elliot and Loudon¹ and the microscopic theory for such a process was described in detail by Fleury and Loudon.² One of the possible mechanisms for the magneto-optical scattering is an indirect electric-dipole (ED) coupling via the spin-orbit interaction, and such a mechanism has been used to determine the spectrum of magnetic excitations in many different condensed matter systems like fluorides, XF_2 , where X is Mn^{2+} , Fe^{2+} , or Co^{2+} ,² inorganic spin-Pierls compounds, CuGeO_3 ,³ and the parent compounds of the high-temperature superconductors, such as La_2CuO_4 .⁴

In this Rapid Communication we report on a theoretical study of the Raman spectrum in a two-dimensional (2D) quantum Heisenberg antiferromagnet (QHAF) with Dzyaloshinskii-Moryia (DM) and XY interactions, which is a model for the magnetism of a single layer in La_2CuO_4 . As it was recently shown in Ref. 5, although small, such anisotropic DM and XY terms are very important in order to explain the unusual magnetic-susceptibility anisotropies observed in La_2CuO_4 .⁶ It was found, in particular, that, below the Néel ordering temperature, T_N , the two transverse magnon modes are gapped, with their respective gaps being uniquely determined by the strength of the DM and XY interaction terms, in agreement with neutron scattering experiments.⁷ However, more recent Raman-spectroscopy experiments reported on the presence of *only one* of the above two magnon modes, the DM mode, in the Raman spectrum for the planar (RL) geometry (R =right rotating and L =left rotating) at zero magnetic field.⁴ Most surprisingly, it was also found that a second mode can be induced in the *forbidden* (RR) geometry, for a magnetic field applied along the easy axis for the staggered magnetization, and only for such configuration. As we now clarify, the appearance of such a field-induced mode (FIM) is directly associated to a continuous rotation of the spin quantization basis, which modifies the selection rules set by the ED coupling on the Raman scattering cross section, thus allowing for the observation of the, previously selected out, XY magnon mode in the spectrum.

The Hamiltonian representing the interaction of light with magnons can be written quite generally as⁸

$$H_{ED} = \sum_{\mathbf{r}} \mathbf{E}_S^T \chi(\mathbf{r}) \mathbf{E}_I, \quad (1)$$

where \mathbf{E}_S and \mathbf{E}_I are the electric fields of the scattered and incident radiation, respectively (\mathbf{a}^T is the transposed of the \mathbf{a} vector) and $\chi(\mathbf{r})$ is the spin-dependent susceptibility tensor. We can expand $\chi(\mathbf{r})$ in powers of the spin operators, \mathbf{S} , as

$$\chi^{\alpha\beta}(\mathbf{r}) = \chi_0^{\alpha\beta}(\mathbf{r}) + \sum_{\mu} K_{\alpha\beta\mu} S^{\mu}(\mathbf{r}) + \sum_{\mu\nu} G_{\alpha\beta\mu\nu} S^{\mu}(\mathbf{r}) S^{\nu}(\mathbf{r}) + \dots, \quad (2)$$

where $\mu, \nu = x, y, z$ label the spin components. The lowest-order term $\chi_0^{\alpha\beta}(\mathbf{r})$ is just the susceptibility in the absence of any magnetic excitation (it corresponds to elastic scattering), and it will be neglected in what follows. The second and third terms can give rise to one-magnon excitations because they can be written as $S^{\pm}(\mathbf{r})$ and $S^z(\mathbf{r})S^{\pm}(\mathbf{r})$, respectively. The intensity of the scattering, as well as the selection rules, will be determined by the structure of the complex tensors K and G . For a square-lattice antiferromagnet, the linear term on the spins reduces to (for Stokes scattering only)

$$H_{ED}^{AS} = iK_0 \sum_{i_A, i_B} [(E_3^z E_I^+ - E_3^+ E_I^z) S_{i_A}^- - (E_3^z E_I^- - E_3^- E_I^z) S_{i_B}^+], \quad (3)$$

where the sum runs over the two sublattices A and B , the K_0 coupling constant is the same for the two sublattices, and z is the direction of the spin easy axis.⁸ Analogously, the quadratic term on the spins reduces to

$$H_{ED}^S = G_0 \sum_{i_A, i_B} [(E_3^z E_I^+ + E_3^+ E_I^z) O_{i_A}^- + (E_3^z E_I^- + E_3^- E_I^z) O_{i_B}^+], \quad (4)$$

where G_0 is a coupling constant and $O_i^{\pm} = S_i^z S_i^{\pm} + S_i^{\pm} S_i^z$.⁸ We see that while the K tensor is purely imaginary and totally antisymmetric, the G tensor is purely real and totally symmetric, as required by the general symmetry properties of the electric susceptibility of a magnetic material, also known as Onsager relations.⁹ Furthermore, the relative values of the coupling coefficients, K_0 and G_0 , can be deduced from the measure-

ments of magneto-optical effects such as magnetic circular birefringence (to determine K_0) and magnetic linear birefringence (to determine G_0).⁸

The total ED Hamiltonian $H_{ED} = H_{ED}^{AS} + H_{ED}^S$ can be finally written in terms of the x, y, z components of the sublattice magnetization, $\mathbf{M}_i = (\mathbf{S}_{i_A} - \mathbf{S}_{i_B})/2$, as

$$H_{ED} = \sum_i \{ \mathbf{E}_S^T \chi^x \mathbf{E}_I M_i^x + \mathbf{E}_S^T \chi^y \mathbf{E}_I M_i^y \}, \quad (5)$$

where we introduced the matrices

$$\chi^x = \begin{pmatrix} 0 & 0 & d \\ 0 & 0 & 0 \\ d^* & 0 & 0 \end{pmatrix}, \quad \chi^y = \begin{pmatrix} 0 & 0 & 0 \\ 0 & 0 & d \\ 0 & d^* & 0 \end{pmatrix},$$

with $d = G_0 S + iK_0$. Here we made the usual mean-field assumption $\langle S_{i_A}^z \rangle = -\langle S_{i_B}^z \rangle = -S$ and we dropped terms of the type $S_{i_A}^{x,y} + S_{i_B}^{x,y}$ since these will give rise to a negligible contribution for the $\mathbf{k}=0$ scattering in the long-wavelength limit. In deriving Eq. (5) we assumed that the spins order along the z direction. In the more general case, the spin easy axis is along a different direction \tilde{z} with respect to a given (x, y, z) reference system (for example, the one attached to the unit cell of the crystal). In this case, one should rewrite the ED Hamiltonian as

$$H_{ED} = \sum_i \{ \mathbf{E}_S^T \tilde{\chi}^x \mathbf{E}_I \tilde{M}_i^x + \mathbf{E}_S^T \tilde{\chi}^y \mathbf{E}_I \tilde{M}_i^y \}, \quad (6)$$

where $\tilde{\chi}^{x,y} = R^T \chi^{x,y} R$, $\tilde{\mathbf{M}} = R \mathbf{M}$, and R is the matrix of the rotation from (x, y, z) to $(\tilde{x}, \tilde{y}, \tilde{z})$.

The above Hamiltonian (5) is to be treated as a perturbation of the following single-layer $S=1/2$ Hamiltonian for the La_2CuO_4 system

$$H_S = J \sum_{\langle i,j \rangle} \mathbf{S}_i \cdot \mathbf{S}_j + \sum_{\langle i,j \rangle} \mathbf{D}_{ij} \cdot (\mathbf{S}_i \times \mathbf{S}_j) + \sum_{\langle i,j \rangle} \mathbf{S}_i \cdot \tilde{\Gamma}_{ij} \cdot \mathbf{S}_j, \quad (7)$$

where J is the in-plane antiferromagnetic (AF) superexchange between the spins, \mathbf{S}_i , of the neighboring Cu^{2+} ions, and \mathbf{D}_{ij} and $\tilde{\Gamma}_{ij}$ are, respectively, the DM and XY anisotropic interaction terms of the low temperature orthorhombic (LTO) phase of La_2CuO_4 .¹⁰ The long-wavelength effective theory for the Hamiltonian (7) was derived in Ref. 5. As usual, one decomposes the Cu^{2+} spins in their staggered, \mathbf{n} , and uniform, \mathbf{L} , components as: $\mathbf{S}_i(\tau) = e^{i\mathbf{Q} \cdot \mathbf{x}_i} \mathbf{n}(\mathbf{x}_i, \tau) + \mathbf{L}(\mathbf{x}_i, \tau)$, where $\mathbf{Q} = (\pi, \pi)$, and one then integrates out \mathbf{L} to obtain

$$S = \frac{1}{2g_0 c_0} \int_0^\beta d\tau \int d^2\mathbf{x} \{ (\partial_\tau \mathbf{n} + i\mathbf{B} \times \mathbf{n})^2 + c_0^2 (\nabla \mathbf{n})^2 + (\mathbf{D}_+ \cdot \mathbf{n})^2 + \Gamma_c (n^c)^2 + 2\mathbf{B} \cdot (\mathbf{D}_+ \times \mathbf{n}) \}, \quad (8)$$

where $\mathbf{n}(\mathbf{x}, \tau)$, the continuum analogous of \mathbf{M}_i , is required to satisfy $\mathbf{n}^2 = 1$. Here g_0 is the bare coupling constant, related to the spin-wave velocity, c_0 , and renormalized stiffness, ρ_s , through $\rho_s = c_0(1/Ng_0 - \Lambda/4\pi)$,⁵ Λ is a cutoff for momentum integrals (we set the lattice spacing $a=1$), $N=3$ is the number of spin components, $\mathbf{D}_+ = D_+ \hat{\mathbf{x}}_a$, and $\Gamma_c > 0$. From now on we will use the LTO (a, b, c) coordinate system of Fig. 1, where $\hat{\mathbf{x}}_a$, $\hat{\mathbf{x}}_b$, and $\hat{\mathbf{x}}_c$ are the LTO unit vectors. From Eq. (8) it

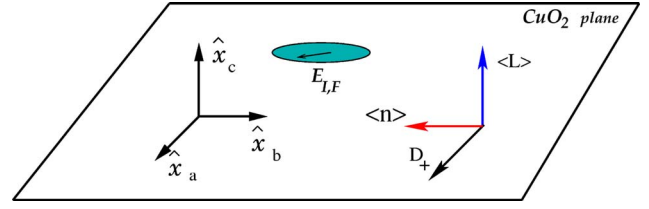


FIG. 1. (Color online) Left: LTO coordinate system with respect to a single CuO_2 layer. Right: direction of the staggered magnetization, $\langle \mathbf{n} \rangle$, of the DM vector, \mathbf{D}_+ , and of the WFM, $\langle \mathbf{L} \rangle \propto \langle \mathbf{n} \rangle \times \mathbf{D}_+$, for $\mathbf{B}=0$. In the scattering geometry of Ref. 4, the electric field vector of the light, $\mathbf{E}_{I,F}$, is always parallel to the ab plane.

follows that the two transverse staggered modes n^a and n^c have their gaps given by $\Delta_a = D_+ = 2.5$ meV and $\Delta_c = \sqrt{\Gamma_c} = 5$ meV, respectively, so that $\hat{\mathbf{x}}_b$ is the easy axis for the staggered magnetization. Since the uniform magnetization $\langle \mathbf{L} \rangle = (1/2J) \langle \langle \mathbf{n} \rangle \times \mathbf{D}_+ \rangle$,⁵ we find that, in the ordered AF phase (for $\mathbf{B}=0$), a nonzero weak-ferromagnetic moment (WFM) $\langle \mathbf{L} \rangle$ is present, directed along $\hat{\mathbf{x}}_c$ [see Figs. 1 and 2(a)].

We can now discuss the experiments of Gozar *et al.*⁴ in the absence of magnetic field, $\mathbf{B}=0$. First, let us observe that since the sublattice magnetization, $\langle \mathbf{n} \rangle$, is oriented along the LTO \mathbf{x}_b direction, the Hamiltonian (5) reads in the continuum

$$H_{ED} = \int d^2\mathbf{x} \{ \mathbf{E}_S^T \chi^a \mathbf{E}_I n^a + \mathbf{E}_S^T \chi^c \mathbf{E}_I n^c \} = \int d^2\mathbf{x} \{ \Pi_a n^a + \Pi_c n^c \}, \quad (9)$$

where we have introduced the polarization projectors $\Pi_{a,c} = \mathbf{E}_S^T \chi^{a,c} \mathbf{E}_I$ with

$$\chi^a = \begin{pmatrix} 0 & d & 0 \\ d^* & 0 & 0 \\ 0 & 0 & 0 \end{pmatrix}, \quad \chi^c = \begin{pmatrix} 0 & 0 & 0 \\ 0 & 0 & d \\ 0 & d^* & 0 \end{pmatrix}, \quad (10)$$

in the LTO abc coordinate system. The structure of the above matrices implies immediately that the n^a (DM) and n^c (XY) modes should be observed, respectively, in the B_{1g} and B_{3g} channels of the nonmagnetic B_{mab} orthorhombic group of the LTO phase of La_2CuO_4 .

The Brillouin zone center one-magnon Raman intensity can now be calculated from Fermi's golden rule using the Hamiltonian (9) as a perturbation, and we obtain, for Stokes scattering,

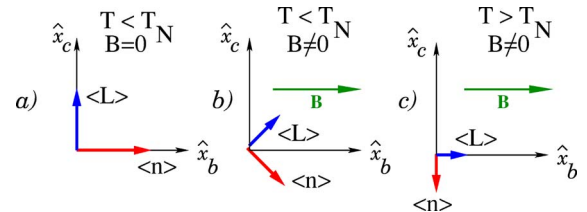


FIG. 2. (Color online) Orientation of the staggered magnetization $\langle \mathbf{n} \rangle$ and of the WFM $\langle \mathbf{L} \rangle$ for: (a) zero field $\mathbf{B}=0$; (b) $\mathbf{B} < \mathbf{B}_c$ and $T < T_N$ (θ and $\langle \mathbf{n} \rangle$ are functions of T); and (c) $\mathbf{B} < \mathbf{B}_c$ and $T > T_N$. Observe that (c) is also realized at any T for $\mathbf{B} > \mathbf{B}_c$.

$$\mathcal{I}(\omega) = [n_B(\omega) + 1] \{ |\Pi_a|^2 \mathcal{A}_a(\mathbf{0}, \omega) + |\Pi_c|^2 \mathcal{A}_c(\mathbf{0}, \omega) \}, \quad (11)$$

where $n_B(\omega) = (e^{\beta\omega} - 1)^{-1}$ is the Bose function and $\mathcal{A}_{a,c}(\mathbf{0}, \omega)$ is the $\mathbf{q}=0$ spectral function of the transverse modes, which is peaked at the mass value $\Delta_{a,c}$.

The scattering geometry used in Ref. 4 is the so-called *backscattering* geometry. In this setting, the direction of the propagating wave vectors of both the incoming and outgoing radiations are chosen to be along $\hat{\mathbf{x}}_c$, in such a way that the electric field of the light is always parallel to the CuO_2 or ab plane (see Fig. 1). Let us denote by $(\hat{e}_{in}\hat{e}_{out})$ the polarization configurations. Two polarization configurations were used in Ref. 4: (i) light linearly polarized with $\hat{e}_m = \hat{\mathbf{x}}_a$ and $\hat{e}_{out} = \hat{\mathbf{x}}_b$ (B_{1g} geometry); and (ii) light right/left circularly polarized, $\hat{e}^R = (1/\sqrt{2})(\hat{\mathbf{x}}_a - i\hat{\mathbf{x}}_b)$, and $\hat{e}^L = (1/\sqrt{2})(\hat{\mathbf{x}}_a + i\hat{\mathbf{x}}_b)$, combined in the (RL) or (RR) geometries. It is worth mentioning at this point that the (RL) and (RR) polarization configurations probe, respectively, the antisymmetric (imaginary) and symmetric (real) parts of the Raman tensor χ^a in (10), i.e., $\Pi_a^{RL} = 2iK_0$ and $\Pi_a^{RR} = 2iG_0S$. Moreover, because the electric field of the light is always parallel to the ab plane, $\Pi_c = 0$ for any polarization configuration. As a result, we find that *only* the spectral function of the n^a mode, $\mathcal{A}_a(\mathbf{0}, \omega)$, which is peaked at the DM gap, Δ_a , contributes to the Raman intensity (11) in the B_{1g} channel, in agreement with the experiments of Ref. 4 for both the B_{1g} and (RL) geometries. We observe, furthermore, that within the ideal microscopic theory of Fléury and Loudon,² one should always have $G_0 = 0$ for magnetic systems in which the ground state has zero or quenched orbital angular momentum. When this happens, also $\Pi_a^{RR} = 0$, in which case we could refer to the (RR) geometry as *forbidden*.

Let us discuss the effects of a magnetic field \mathbf{B} applied along $\hat{\mathbf{x}}_b$, which is the configuration where the FIM is observed in Ref. 4. The first term in Eq. (8) is responsible for the softening of the transverse gaps, by an amount $B^2, \Delta_{a,c}^2 \rightarrow \Delta_{a,c}^2 - B^2$, as observed in the measurements of Ref. 4. However, this softening is quantitatively very small for small fields and will be neglected in what follows. Conversely, the most remarkable effect of the magnetic field comes from the last term in Eq. (8), which can be written as $(1/g_0c_0) \int_0^\beta d\tau \int d^2\mathbf{x} h n_c$, where $h = |\mathbf{B} \times \mathbf{D}_+|$. As we can see, such a term generates, for $B \parallel \hat{\mathbf{x}}_b$, an effective *staggered* field h coupled to n^c , leading to a rotation of the staggered-magnetization order parameter with respect to the zero-field case [see Fig. 2(b)]. In fact, if we write $\langle \mathbf{n} \rangle = (0, \sigma_b, \sigma_c)$ for the order parameter we obtain at mean-field level

$$\sigma_b^2 = 1 - \sigma_c^2 - NI_\perp(\xi = \infty), \quad \sigma_c = -h/\Gamma_c, \quad (12)$$

for $T < T_N$, and

$$\sigma_b = 0, \quad \sigma_c = -h/(\Gamma_c + \xi^{-2}), \quad 1 = \sigma_c^2 + NI_\perp(\xi), \quad (13)$$

for $T > T_N$, where, following the notation of Ref. 5, ξ is the correlation length and $I_\perp = (1/2)(I_a + I_c)$ is the integral of the transverse fluctuations¹¹

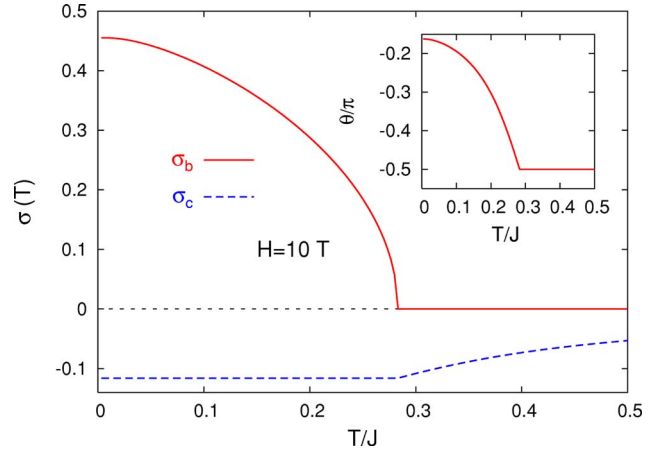


FIG. 3. (Color online) T dependence of σ_b and σ_c at $H=10T$, from Eqs. (12) and (13). Inset: T dependence of the angle θ , from Eq. (14).

$$I_a = \frac{g_0 T}{2\pi c_0} \ln \left\{ \frac{\sinh(c_0 \Lambda / 2T)}{\sinh(\Delta_a / 2T)} \right\}.$$

The temperature dependence of the components of the $\langle \mathbf{n} \rangle$, as well as of the angle θ ,

$$\tan \theta = \frac{\sigma_c}{\sigma_b}, \quad (14)$$

that defines the rotation of $\langle \mathbf{n} \rangle$ from the $\hat{\mathbf{x}}_b$ direction, are reported in Fig. 3. Observe that for $h \neq 0$ we conclude that the uniform magnetization

$$\langle \mathbf{L} \rangle = \frac{D_+}{2J} (|\sigma_b| \hat{\mathbf{x}}_c + |\sigma_c| \hat{\mathbf{x}}_b), \quad (15)$$

is also rotated from its original orientation, perpendicular to the CuO_2 planes, by the same angle θ [see Fig. 2(b)]. Notice, furthermore, that such rotation has the $\hat{\mathbf{x}}_a$ axis as the symmetry axis, in such a way that both $\langle \mathbf{n} \rangle$ and $\langle \mathbf{L} \rangle$ are always confined to the bc plane.⁶ Moreover, the angle of rotation varies continuously from its $T=0$ value until $\theta = -\pi/2$ (see inset of Fig. 3), because $\sigma_b \rightarrow 0$ continuously as $T \rightarrow T_N(B)$. This is a very important finding because it shows clearly that no two-step spin-flop transition occurs, in agreement with magnetoresistance experiments.¹² Finally, as the field \mathbf{B} increases, the $T=0$ value of σ_b decreases, until a critical field \mathbf{B}_c above which the order parameter is always oriented along the $\hat{\mathbf{x}}_c$ direction. As a consequence, either at $T > T_N(\mathbf{B})$, for $\mathbf{B} < \mathbf{B}_c$, or at arbitrary temperature and $\mathbf{B} > \mathbf{B}_c$ we find a new magnetic state with $\sigma_b = 0$ and $\sigma_c \neq 0$, where the WFM is confined to the ab plane and ordered along the $\hat{\mathbf{x}}_b$ LTO direction, as it was suggested by the experiments of Gozar *et al.*⁴ Within our mean-field calculation the critical field \mathbf{B}_c at $T=0$ can be estimated from Eq. (12) as $B_c = \sqrt{1 - Ng\Lambda/4\pi(\Gamma_c/D_+)} = 40 T$.

We are now ready to explain how the above rotation of the spin easy axis, induced by the magnetic field, modifies

the Raman spectra. The matrix R describing the rotation by the angle θ around the $\hat{\mathbf{x}}_a$ direction modifies the Raman matrices (10) to

$$\tilde{\chi}^a = \begin{pmatrix} 0 & d \cos \theta & -d \sin \theta \\ d^* \cos \theta & 0 & 0 \\ -d^* \sin \theta & 0 & 0 \end{pmatrix},$$

$$\tilde{\chi}^c = \begin{pmatrix} 0 & 0 & 0 \\ 0 & (d+d^*)\sin \theta \cos \theta & -d^* \sin^2 \theta + d \cos^2 \theta \\ 0 & -d \sin^2 \theta + d^* \cos^2 \theta & -(d+d^*)\sin \theta \cos \theta \end{pmatrix}. \quad (16)$$

The new transverse spin modes correspond to $\tilde{n}^a = n^a$, since the rotation leaves the $\hat{\mathbf{x}}_a$ direction untouched, and $\tilde{n}^c = n^c \cos \theta + n^b \sin \theta$. Observe that the main effect of the rotation is that now $\Pi_c \propto \mathbf{E}_S^T \tilde{\chi}^c \mathbf{E}_I \neq 0$, so that also the $n_c(XY)$ mode can be observed. More specifically, from Eqs. (6) and (16) it follows that in the (RR) geometry used in Ref. 4 $\Pi_a^{RR} = 2iG_0 \cos \theta$ and $\Pi_c^{RR} = G_0 \sin 2\theta \cos \theta$. As a consequence, now also the spectral function of the n_c mode, $\mathcal{A}_c(\mathbf{0}, \omega)$, contributes to the intensity (11) with a peak at the energy Δ_c , which corresponds to the XY gap. We thus conclude that the FIM mode observed in Ref. 4 is nothing less than the XY mode, which can only be seen for $\mathbf{B} \parallel \hat{\mathbf{x}}_b$ and nonzero G_0 . We should remark at this point that the above

effect occurs only for $\mathbf{B} \parallel \hat{\mathbf{x}}_b$, thus justifying the appearance of the FIM only for that orientation of the magnetic field. In fact, for $\mathbf{B} \parallel \hat{\mathbf{x}}_a$, we have $h=0$ and $\sigma_c=0$. In this case, $\langle \mathbf{n} \rangle = \sigma_b \hat{\mathbf{x}}_b$, and $\langle \mathbf{L} \rangle = (1/2J)D_+ \sigma_b \hat{\mathbf{x}}_c$ [see Fig. 2(a)]. The case of $\mathbf{B} \parallel \hat{\mathbf{x}}_c$ was already discussed in Ref. 5. Although in this third case $h \neq 0$, it is actually a source for the n_b component of the staggered magnetization, and we again have $\sigma_c=0$. Thus, for either $\mathbf{B} \parallel \hat{\mathbf{x}}_a$ or $\mathbf{B} \parallel \hat{\mathbf{x}}_c$, where $\theta=0$, we will have $\Pi_c=0$ and only the DM mode will be present in the one-magnon Raman spectrum.

In conclusion, we have found that the appearance of the FIM for $\mathbf{B} \parallel \mathbf{x}_b$ is a consequence of both a *continuous* rotation of the spin-quantization basis and of a nonzero symmetric part for the χ^c Raman tensor, $G_0 \neq 0$, signaling a deviation from the ideal ED scattering mechanism of Fleury and Loudon.² Furthermore, we have found a magnetic state, well above T_N , in which the WFM is confined to the ab plane. The absolute intensities of the one-magnon Raman peaks in the two circular polarizations, (RL) and (RR) , are given in terms of K_0 and G_0 , which have to be determined from first principles. Moreover, to obtain the temperature and field dependencies of the relative peak intensity of the FIM a more precise calculation of the T and B dependencies of the anisotropy gaps and of the spin damping would be required.

The authors have benefited from invaluable discussions with Y. Ando, G. Blumberg, S. Caprara, A. Gozar, M. Grilli, A. N. Lavrov, and J. Lorenzana.

*Electronic address: m.barbosadasilvaneto@phys.uu.nl

¹R. J. Elliot and R. Loudon, Phys. Lett. **3**, 189 (1963).

²P. A. Fleury and R. Loudon, Phys. Rev. **166**, 514 (1968).

³P. H. M. van Loosdrecht, in *Solid State Phenomena*, edited by M. Davidovic and Z. Ikonc (Trans Tech Publications, Switzerland, 1998), Vol. 61–62, pp. 19–26.

⁴A. Gozar, B. S. Dennis, G. Blumberg, S. Komiyama, and Y. Ando, Phys. Rev. Lett. **93**, 027001 (2004).

⁵M. B. Silva Neto, L. Benfatto, V. Juricic, and C. Morais Smith, cond-mat/0502588 (unpublished).

⁶A. N. Lavrov, Y. Ando, S. Komiyama, and I. Tsukada, Phys. Rev. Lett. **87**, 017007 (2001).

⁷B. Keimer, R. J. Birgeneau, A. Cassanho, Y. Endoh, M. Greven, M. A. Kastner, and G. Shirane, Z. Phys. B: Condens. Matter **91**,

373 (1993).

⁸M. G. Cottam and D. J. Lockwood, *Light Scattering in Magnetic Solids* (Wiley, New York, 1986).

⁹L. D. Landau and E. M. Lifshitz, *Electrodynamics of Continuous Media* (Pergamon, Oxford, 1960).

¹⁰L. Shekhtman, O. Entin-Wohlman, and A. Aharony, Phys. Rev. Lett. **69**, 836 (1992); W. Koshibae, Y. Ohta, and S. Maekawa, Phys. Rev. B **50**, 3767 (1994).

¹¹We fix $\rho_s=0.1J$, $c_0=1.3J$, and $J=100$ meV by fitting the experimental data for the correlation length ξ , with Eq. (13) (see Ref. 5).

¹²Y. Ando, A. N. Lavrov, and S. Komiyama, Phys. Rev. Lett. **90**, 247003 (2003).